Geoscience Frontiers 15 (2024) 101916

Contents lists available at ScienceDirect

Geoscience Frontiers

journal homepage: www.elsevier.com/locate/gsf

Research Paper

Long-term daily water temperatures unveil escalating water warming and intensifying heatwaves in the Odra river Basin, Central Europe

Jiang Sun [a], Fabio Di Nunno [b], Mariusz Sojka [c], Mariusz Ptak [d], Quan Zhou [a], Yi Luo [e], Senlin Zhu [a,*], Francesco Granata [b]

[a] College of Hydraulic Science and Engineering, Yangzhou University, Yangzhou, China
[b] Department of Civil and Mechanical Engineering (DICEM), University of Cassino and Southern Lazio, Via Di Biasio, 43, 03043, Cassino, Frosinone, Italy
[c] Department of Land Improvement, Environmental Development and Spatial Management, Poznań University of Life Sciences, Piątkowska 94E, 60 649 Poznań, Poland
[d] Department of Hydrology and Water Management, Adam Mickiewicz University, B. Krygowskiego 10, 61-680 Poznań, Poland
[e] GIS Technology Research Center of Resource and Environment in Western China, Yunnan Normal University, Kunming, China

ARTICLE INFO

Article history:
Received 5 May 2024
Revised 10 July 2024
Accepted 17 August 2024
Available online 20 August 2024
Handling Editor: S. Kwon

Keywords:
River water temperature
Ensemble modeling
Annual variation
Seasonal pattern
River heatwaves

ABSTRACT

Water temperature is a critical indicator and weathervane of aquatic ecosystems. However, the vast majority of rivers lack long-term continuous and complete water temperature datasets. In this study, ensemble models by combining NARX (nonlinear autoregressive network with exogenous inputs) and air2stream were used to reconstruct daily river water temperatures for 27 hydrological stations in the Odra River Basin, one of the largest river systems in Europe. For each hydrological station, both the NARX and air2stream models were calibrated and validated, and the better-performed model was selected to reconstruct daily river water temperatures from 1985 to 2022. The results showed that hybrid modeling by combining NARX and air2stream is promising for reconstructing daily river water temperatures. Based on the reconstructed dataset, annual and seasonal trends of water temperature and characteristics of river heatwaves were evaluated. The results indicated that annual river water temperatures showed a consistent warming trend over the past 40 years with an average warming rate of 0.315 °C/decade. Seasonal river water temperatures indicated that summer warms faster, followed by autumn and spring, and winter river water temperatures showed an insignificant warming trend. River heatwaves are increased in frequency, duration, and intensity in the Odra River Basin, and 6 out of 27 hydrological stations have river heatwaves categorized as 'severe' and 'extreme', suggesting that mitigation measures are needed to reduce the impact of climate warming on aquatic systems. Moreover, results showed that air temperature is the major controller of river heatwaves, and river heatwaves tend to intensify with the warming of air temperatures.

1. Introduction

Water temperature is a critical factor in aquatic ecosystems, directly impacting the physical, chemical, and biological processes of rivers (Caissie, 2006; Johnson et al., 2024). Escalating global climate change has led to further increases in river water temperatures (RWT), resulting in more frequent and intense river heatwaves with serious impacts on river ecology (Tassone et al., 2023; Zhi et al., 2023a; Johnson et al., 2024; Zhu et al., 2024). To accurately assess river heatwaves, complete and continuous daily data of river water temperatures are essential (Tassone et al., 2023; Zhu et al., 2024).

Many rivers worldwide lack continuous and complete water temperature data, thus using modeling tools to reconstruct daily RWT is popular (e.g., Zhu et al., 2022; Bal and de Eyto, 2023; Huang et al., 2023; Shrestha and Pesklevits, 2023; Zhi et al., 2023b; Shrestha et al., 2024). The choice of an accurate and efficient water temperature prediction model is of paramount importance in this regard.

Many types of models have been proposed for daily RWT prediction in the past decades (e.g., Benyahya et al., 2007; Dugdale et al., 2017; Zhu and Piotrowski, 2020; Qiu et al., 2021; Tao et al., 2021; Almeida and Coelho, 2023; Sun et al., 2024). While simple statistical models can quickly identify water temperature trends,

* Corresponding author.
E-mail address: slzhu@yzu.edu.cn (S. Zhu).

https://doi.org/10.1016/j.gsf.2024.101916

they often lack predicting accuracy (e.g., Stefan and Preud'homme, 1993; Mohseni and Stefan, 1999; Benyahya et al., 2007). Process-based models, favored for their robust physical mechanisms, demand extensive and complex data for model development, making them impractical for many rivers worldwide (e.g., Wright et al., 2009; Dugdale et al., 2017). In recent years, machine learning (ML) models have emerged as potent tools for RWT prediction and reconstruction (e.g., Feigl et al., 2021; Qiu et al., 2021; Tao et al., 2021; Almeida and Coelho, 2023; Sun et al., 2024; Zhu et al., 2024). ML-based models can autonomously explore data interrelationships, establishing intricate connections to achieve precise predictions. Among these ML-based models, NARX-based models (nonlinear autoregressive network with exogenous inputs) have demonstrated their efficiency and accuracy in daily RWT modeling (e.g., Sun et al., 2024; Zhu et al., 2024), especially considering the accuracy of capturing river heatwaves (Zhu et al., 2024).

Previous studies often used a single model to reconstruct daily RWT. For example, Zhu et al. (2022), Shrestha and Pesklevits (2023) and Shrestha et al. (2024) employed the widely used air2stream model to reconstruct daily RWT in Polish and Canadian rivers respectively; Bal and de Eyto (2023) used simple Bayesian reconstruction in two European rivers; Huang et al. (2023) and Zhi et al. (2023b) used deep learning model for Chinese and US rivers. To improve prediction reliability and avoid the limitations of a single model, ensemble modeling by combining multiple models is a good strategy and has become popular in hydrological studies (e.g., Duan et al., 2007; Velázquez et al., 2010; Dion et al., 2021; Olsson et al., 2024). However, to the best of our knowledge, ensemble modeling considering hybrid models has rarely been used to reconstruct daily RWT.

To fill the above gaps, the NARX-based model and air2stream model were ensembled to reconstruct daily river water temperatures for 27 hydrological stations in the Odra River Basin, one of the largest river systems in Europe. For each hydrological station, both the NARX and air2stream models were calibrated and validated, and the better-performed model was selected to reconstruct daily river water temperatures from 1985 to 2022. Based on the reconstructed dataset, annual and seasonal trends of water temperature, and characteristics of river heatwaves, were evaluated. The objectives of this study are (i): to reconstruct daily water temperatures for 27 hydrological stations in the Odra River Basin from 1985 to 2022; (ii) to analyze annual and seasonal variations of river water temperatures for each hydrological station; (iii) to analyze the characteristics of river heatwaves, including the total number, duration, and intensity for each hydrological station. This study will deepen our understanding of the trends of river water temperatures and heatwaves in Poland over the past four decades and provide valuable resources for future studies on river thermal dynamics and environmental management.

2. Materials and methods

2.1. Study area

The Oder River Basin is one of Europe's largest river systems, claiming the 15th spot in terms of area. With a discharge density of 17.3 (km^3/year) and a population density of 134 persons/km^2, it harbors a dynamic landscape shaped significantly by human activities, including urbanization, agriculture, and pastureland, which collectively occupy 60.8% of the region (Tockner et al., 2022). Encompassing territories across three countries—Poland, Germany, and the Czech Republic—it holds the largest expanse within Poland, occupying over 30% of the nation's territory (Fig. 1).

Situated in the heart of Europe, the Oder River Basin experiences a temperate climate marked by transitional traits. Caught between the influence of maritime air masses from the Atlantic and drier currents originating from deep within the Eurasian continent, the region exhibits climatic nuances that shape its ecological and environmental dynamics.

Beyond its ecological significance, the Oder River Basin serves as a vital conduit for inland transportation, boasting numerous waterways that facilitate trade and connectivity. Furthermore, the area is witnessing a surge in tourism development, underscoring its growing importance as a destination for leisure and recreation.

The Oder River itself is 855 km long, its sources are located in the Czech Republic at 634 m a.s.l., and it flows into the Szczecin Lagoon (a bay of the Baltic Sea).

2.2. Data

The dataset utilized in this study comprises measurements conducted as part of the ongoing hydrological monitoring efforts in Poland by the Institute of Meteorology and Water Management (IMWM). These measurements, recorded on a daily basis, encompass water temperature readings taken consistently beneath the water surface at a depth of 0.4 m, precisely at 6 UTC, and at fixed locations marked by water gauges.

However, it is noteworthy that following the reorganization of IMWM's measurement network, the majority of stations ceased stationary water temperature measurements in 2014 (as delineated in Table 1). Nonetheless, for continuity and comprehensiveness, air temperature data sourced from standard meteorological observations have been drawn from IMWM resources.

Furthermore, to ensure precision and relevance to specific rivers under investigation, meteorological measurements from the nearest stations have been incorporated into the analysis (refer to Table 1 and Fig. 1 for details).

2.3. Models

2.3.1. air2stream

The air2stream model is a lumped, semi-empirical and hybrid model for the forecasting of daily RWT (Toffolon and Piccolroaz, 2015). In contrast to the traditional process-based models, the basic physical equation of the model is derived by Talyor expanding the heat budget equation, employing air temperature as the substitute of the net heat flux term. This process simplifies the complex water temperature formula into a simple equation based on air temperature and eight model parameters, resulting in the 8-parameter version (Eq. (1)) of the air2stream model.

$$\frac{dT_w}{dt} = \frac{1}{\theta^{a_4}}\left\{a_1 + a_2T_a - a_3T_w + \theta(a_5 + a_6 cos(2\pi(\frac{t}{t_y} - a_7)) - a_8T_w)\right\} \quad (1)$$

where T_w is daily river water temperature, t is time step, T_a is daily air temperature, t_y is the duration of one year (365 days), θ is the dimensionless discharge, and a_1–a_8 are model parameters.

In addition, the 8-parameter version can be further simplified into the 5-parameter version to reduce computational requirements. Previously, Sun et al. (2024) found that the 5-parameter version had the best modeling performance in Polish rivers. Therefore, in this study, the 5-parameter version of the airstream model was selected to model and reconstruct RWT as Eq. (2).

$$\frac{dT_w}{dt} = \left\{a_1 + a_2T_a - a_3T_w + a_6 cos(2\pi(\frac{t}{t_y} - a_7))\right\} \quad (2)$$

The advantage of this model version is that it only requires air temperature data as the sole model input and automatically searches for the optimal model parameters through the Particle Swarm Optimization algorithm.

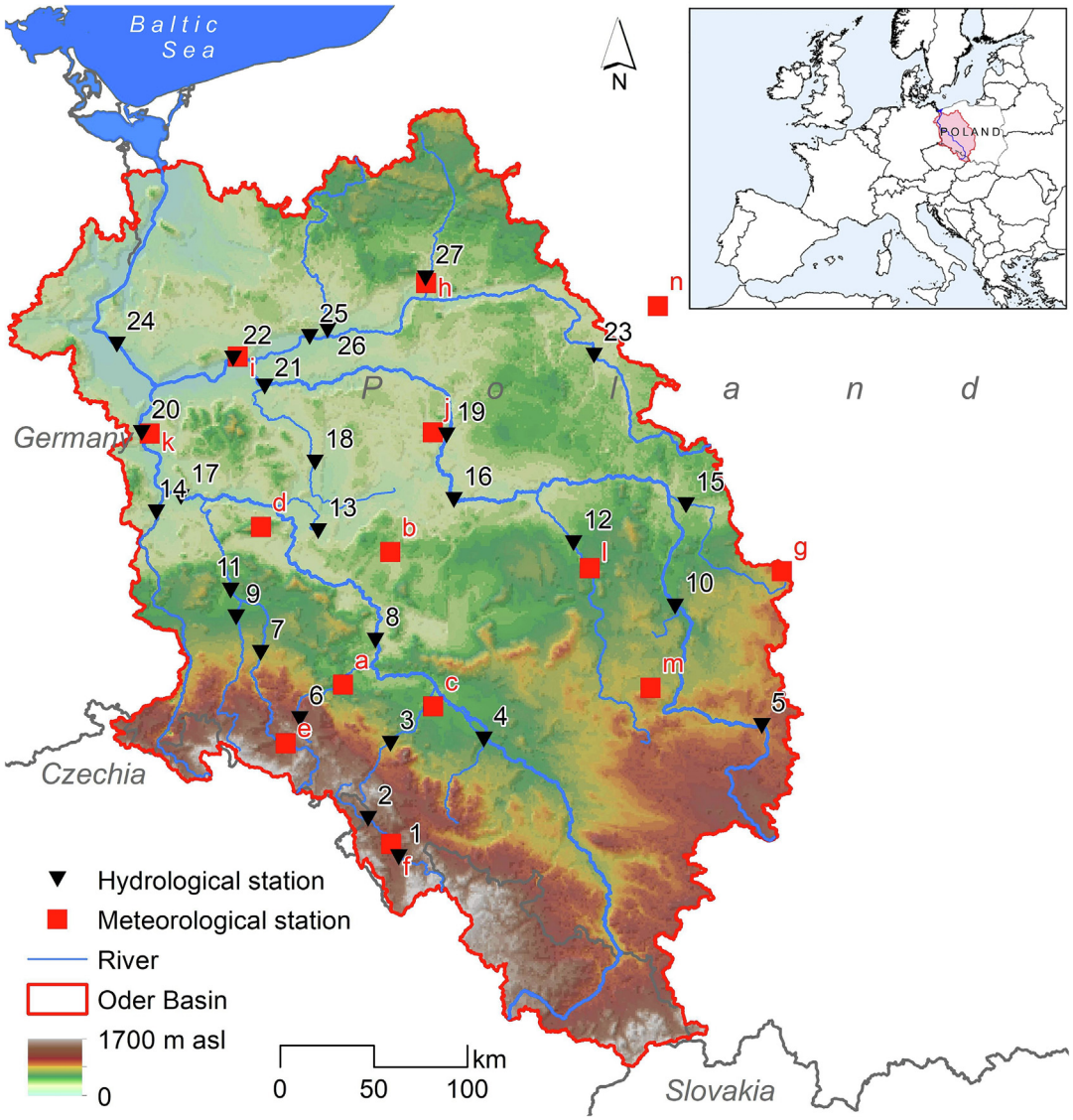

Fig. 1. Locations of the 27 hydrological stations and the corresponding meteorological stations. The numbers and characters are corresponded with that list in Table 1.

2.3.2. NARX networks

This section offers an in-depth overview of the BO-NARX-BR model, highlighting the NARX algorithm utilized for forecasting and the Bayesian Optimization (BO) and Bayesian Regularization (BR) algorithms applied for model tuning. The structure of the NARX model is depicted as Eq. (3):

$$y(t) = f(y(t-1), y(t-2), \cdots, y(t-f_d), x(t-1), x(t-2), \cdots, x(t-p_d)) \quad (3)$$

with $x(t)$ as the exogenous input layer, represented by air temperature and day of the year (DOY), and $y(t)$ as the target, represented by the river water temperature, at a given time t. Moreover, p_d and f_d indicate the lagged values of inputs and target, respectively. Choice of the exogenous variables (air temperature and DOY) in this study followed the conclusion in a recent study at the Vistula River Basin in Europe, indicating that this input combination can produce the best performance for daily RWT modeling using NARX model (Sun et al., 2024).

The NARX structure comprised three different layers (Fig. 2). The initial layer acts as the input, taking in the input parameters. The second layer serves as the hidden layer, handling computations between input and output. Lastly, the third layer operates as the output, delivering the predicted values. Moreover, the predicted output feeds back as input for iterative calculations in the subsequent time step (dot-dash red line in Fig. 2). A sigmoid activation function (f_1) was implemented within the hidden layer, as it's particularly effective for training neural networks using backpropagation methods. This sigmoid function is also differentiable, aiding in the neural network weight learning process. A linear activation function (f_2) was used for the output layer with a single neuron (n). The linear activation function in the output layer allows the model to produce unbounded real values, which aligns well with regression goals. Additionally, the linear activation function is simple and doesn't introduce non-linearity. This straightforwardness, combined with the use of a single neuron, is beneficial for the output layer, particularly when the task requires straightforward predictions without complex transformations (Zhu et al., 2024).

Nonetheless, a key challenge in crafting any forecasting model lies in the thoughtful selection of input variables. In this study, determining the optimal number of lagged values for variables and fine-tuning the hyperparameters for the NARX model were achieved using the BO algorithm (Zhu et al., 2023; Sun et al., 2024). The BO algorithm was specifically used to identify the optimal values for the number of hidden nodes and the lagged values of inputs and target variables. The BO process sets up an objective

Table 1
Detailed information on the studied rivers and analyzed hydrological and meteorological stations. The numbers of the hydrological stations and the characters of the meteorological stations are shown in Fig. 1.

Station No.	Station name	River	Longitude (°E)	Latitude (°N)	Altitude (m a.s.l.)	RWT period	Corresponding meteorological station
1	ŻELAZNO	BIAŁA LĄDECKA	16.403	50.222	316.766	1985–2014	f
2	TŁUMACZÓW	ŚCINAWKA	16.261	50.331	340.151	1985–2014	f
3	KRASKÓW	BYSTRZYCA	16.350	50.546	176.281	1985–2014	c
4	OŁAWA	OŁAWA	17.173	50.565	124.826	1985–2014	c
5	BOBRY	WARTA	19.242	51.013	205.499	1985–2022	m
6	ŚWIERZAWA	KACZAWA	15.532	51.010	256.347	1985–2014	e
7	DĄBROWA BOLESŁAWIECKA	BÓBR	15.341	51.193	157.637	1985–2014	a
8	ŚCINAWA	ODRA	16.264	51.243	86.725	1985–2014	a
9	ŁOZY	KWISA	15.221	51.293	117.336	1985–2014	d
10	SIERADZ	WARTA	18.443	51.356	125.102	1985–2014	l
11	ŻAGAŃ	BÓBR	15.186	51.371	91.914	1985–2014	d
12	BOGUSŁAW	PROSNA	17.571	51.535	87.904	1985–2014	l
13	LUBIATÓW	OBRZYCA	15.581	51.552	52.854	1985–2009	b
14	GUBIN	NYSA ŁUŻYCKA	14.423	51.582	37.607	1985–2014	k
15	DĄBIE	NER	18.493	52.051	93.39	1985–2014	g
16	ŚREM	WARTA	17.010	52.054	57.835	1985–2014	b
17	POŁĘCKO	ODRA	14.533	52.031	32.621	1985–2014	d
18	ZBĄSZYŃ	OBRA	15.552	52.150	50.352	1985–2009	d
19	POZNAŃ-MOST ROCHA	WARTA	16.564	52.241	49.458	1985–2009	j
20	SŁUBICE	ODRA	14.332	52.205	17.446	1985–2014	k
21	SKWIERZYNA	WARTA	15.300	52.361	21.817	1985–2010	i
22	GORZÓW WIELKOPOLSKI	WARTA	15.151	52.435	15.514	1985–2009	i
23	PAKOŚĆ	NOTEĆ	18.054	52.480	72.763	1985–2014	n
24	GOZDOWICE	ODRA	14.190	52.455	3.02	1985–2014	i
25	NOWE DREZDENKO	NOTEĆ	15.502	52.510	24.208	1985–2014	i
26	DRAWINY	DRAWA	15.584	52.531	29.79	1985–2014	i
27	PIŁA	GWDA	16.443	53.091	54.426	1985–2014	h

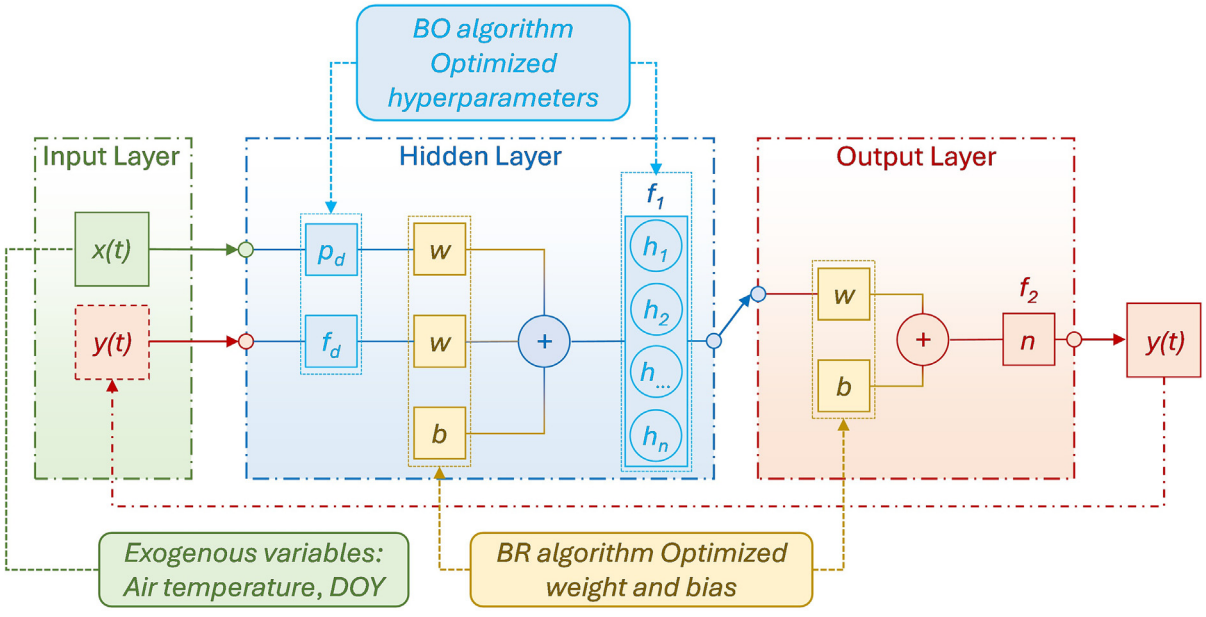

Fig. 2. Sketch of the BO-NARX-BR model.

function for Bayesian optimization and outlines the hyperparameter search space, which includes the number of hidden nodes, lags, and delays. Following this, the NARX model undergoes iterative training and evaluation, yielding a loss value expressed as Mean Square Error (MSE) for each hyperparameter combination. Hence, the values for the number of hidden nodes, p_d, and f_d that minimize MSE were deemed optimal for the modeling.

Additionally, other NARX parameters require calibration. Among them, the weight (w) and bias (b) parameters are influenced by the selected training algorithm. In this study, the BR back-propagation training algorithm (MacKay, 1992; Foresee and Hagan, 1997) was chosen. This algorithm outperformed both Levenberg-Marquardt (LM) and Scaled Conjugate Gradient (SCG) algorithms, which were preliminarily tested. The superiority of the BR algorithm is consistent with prior research in the field, indicating that BR may have slower convergence but offers superior performance compared to LM and SCG (Di Nunno et al., 2022; Zhu et al., 2023, 2024).

Finally, the BO-NARX-BR process was stopped when any of the following conditions were met:

(i) reaching the maximum number of epochs (set to 1000);
(ii) achieving the LM adjustment parameter (set at 1×10^{10});
(iii) reaching an error gradient below a set threshold (set at 1×10^{-7}).

The BO-NARX-BR model was implemented using the MATLAB environment (refer to the Data and Code Availability section for further details).

2.3.3. Model setup and evaluation

In this study, as for most hydrological stations, the available RWT datasets span from 1985 to 2014 (Table 1), they were divided into training (1985–2005) and testing (2006–2014) sets. For the other hydrological stations only having data from 1985 to 2009, data from 1985 to 2002 were used for model training, and the remaining data were used for model testing. Note that for one hydrological station-Bobry, on the Warta River, the RWT time series is from 1985 to 2022, and data from 1985 to 2010 were used for training and the remaining data were used for testing. For model input, air temperature and DOY were used as exogenous variables as mentioned above, and for all the meteorological stations, daily air temperatures span from 1985 to 2022.

To assess the model performance, three widely used evaluated metrics were employed: Nash-Sutcliffe efficiency coefficient (NSE), root mean squared error (RMSE), and mean absolute error (MAE) as Eqs. (4)–(6).

$$\mathrm{NSE} = 1 - \frac{\sum_{i=1}^{n}\left(T_M^i - T_O^i\right)^2}{\sum_{i=1}^{n}\left(T_O^i - \bar{T}\right)^2} \tag{4}$$

$$\mathrm{RMSE} = \sqrt{\frac{\sum_{i=1}^{n}\left(T_M^i - T_O^i\right)^2}{n}} \tag{5}$$

$$\mathrm{MAE} = \frac{1}{n}\sum_{i=1}^{n}\left|T_M^i - T_O^i\right| \tag{6}$$

where T_M^i and T_O^i are modelled and observed river water temperatures for the i^{th} data, $\bar{T}$ is the average value of T_O^i, and n is the number of samples.

Table 2 summarizes the model parameters for the NARX-based model (number of hidden nodes and delays computed based on the BO process) and the air2stream model (a_1, a_2, a_3, a_6, and a_7 determined by the particle swarm optimization algorithm).

2.4. Computation of river heatwaves

River heatwaves are identified to occur when daily river water temperatures are above a local and seasonally varying 90th percentile threshold, which was produced by computing the daily 90th percentile of daily river water temperatures using an 11-day window centered on the day of year over a baseline (30 years, 1985–2014) as suggested by Hobday et al. (2016). As defined, as a river heatwave event, the 90th percentile threshold has to be exceeded for at least five consecutive days, and two events with a break of less than three days are considered as a single heatwave event. Characteristics of heatwaves are computed based the Python program in Hobday et al. (2016), which was initially used for marine heatwaves, and was used in the computation of lake and river heatwaves in subsequent studies (e.g., Woolway et al., 2021; Di Nunno et al., 2023; Tassone et al., 2023; Wang et al., 2023; Zhu et al., 2023; 2024). The characteristics of river heatwaves include total number (times), duration (days), intensity (°C), and category. The category of river heatwaves includes four groups based on the maximum intensity in multiples of threshold exceedances as defined in Hobday et al. (2016): moderate (M), strong (S), severe (SE), and extreme (E).

3. Results

3.1. Model performance

The performance metrics of the two models across all the hydrological stations are presented in Supplementary Data Tables S1 and S2, and results of the better-performed model are presented in Table 3 in detail. As seen, the NARX-based model outperformed the air2stream model for 18 out of the 27 hydrological stations, and for the remaining 9 hydrological stations, the air2stream model performed better.

Fig. 3 displays the time series of RWT and AT, encompassing the training, testing, and reconstructed time periods, for both the Oława (Fig. 3) and Poznań (Fig. 3) stations. In particular, for the Oława station, RWT data were available until 2014, and the best performance was achieved with the NARX-based model. Conversely, for the Poznań station, RWT data were available until 2009, and the best performance was attained with the air2stream-based model. However, in both cases, during the reconstruction period up to 2022, peaks of RWT equal to or higher than those during the training and testing periods can be observed. This is attributed to the utilization of air temperature as an exogenous input variable. As will be discussed further in the next sections, the air temperature has shown increasing trends from 1985 to the present, involving a reconstruction of RWT consistent with these trends.

Moreover, the performance of the two models in six hydrological stations during the testing period was represented as measured vs. predicted values in Fig. 4. As observed, both BO-NARX-BR and air2stream yielded accurate predictions, with the points distributed quite symmetrically around the 1:1 line, not significantly deviating from it. This indicates a balanced performance with similar occurrences of overestimations and underestimations of RWT by both models across the dataset.

Concerning the detailed model performance, as shown in Table 3, during the calibration period, RMSE ranged between 0.615 °C and 2.168 °C with an average value of 1.165 °C, NSE ranged between 0.856 and 0.991 (average: 0.961), and MAE varied between 0.463 °C and 1.619 °C (average: 0.878 °C). In the validation period, RMSE ranged between 0.492 °C and 1.892 °C (average: 1.129 °C), NSE ranged from 0.870 to 0.995 (average: 0.965), and MAE varied from 0.385 °C to 1.371 °C (average: 0.859 °C). The results suggest the excellent predictive performance of the ensemble modeling, demonstrating its suitability for reconstructing river water temperatures. Therefore, the better-performed model selected for each hydrological station was used to reconstruct daily water temperatures from 1985 to 2022.

3.2. Annual and seasonal trends of river water temperatures

Annual and seasonal warming rates (°C/decade) of river water temperatures and air temperatures are summarized in Table 4. Fig. 5 shows the warming rates of river water temperatures (blue arrows) and air temperatures (red arrows). Four seasons are defined as spring (April–June), summer (July–September), autumn (October–December), and winter (January–March). As winter RWT showed an insignificant trend for all hydrological stations, only the results of the other three seasons are included in Table 4.

As seen, the annual averaged RWT in 25 out of 27 hydrological stations showed a clear warming trend ($p < 0.05$) following the warming of air temperature, with the warming rate ranging from 0.054 °C/decade (No. 2) to 0.544 °C/decade (No. 4) (average:

Table 2
Summary of model parameters of the better performed model for each hydrological station. The station No. corresponds with that list in Table 1. Note that for each hydrological station, only the parameters of the better performed model are provided.

Station No.	NARX		air2stream				
	Hidden nodes	Delays	a_1	a_2	a_3	a_6	a_7
1	10	13					
2	23	14					
3	47	13					
4	77	14					
5	40	12					
6	99	9					
7	98	7					
8	10	11					
9			4.191	0.156	0.633	2.943	0.587
10	12	14					
11	93	14					
12	10	14					
13			2.029	0.141	0.303	1.765	0.569
14			2.160	0.113	0.307	1.770	0.551
15	64	8					
16	50	9					
17			2.029	0.141	0.303	1.765	0.569
18			1.596	0.194	0.323	1.371	0.544
19			0.502	0.140	0.170	0.441	0.506
20	78	14					
21			0.959	0.206	0.273	0.800	0.524
22			1.193	0.230	0.316	1.003	0.530
23	40	12					
24	100	14					
25	98	14					
26			2.053	0.145	0.352	1.666	0.549
27	11	14					

Table 3
The performance metrics of the better performed model for each hydrological station. The station No. corresponds with that list in Table 1. A2S refers to the air2stream model.

Station No.	Calibration			Validation			Selected model
	NSE	RMSE (°C)	MAE (°C)	NSE	RMSE (°C)	MAE (°C)	
1	0.944	1.175	0.932	0.934	1.263	0.946	NARX
2	0.856	2.168	1.619	0.938	1.284	1.008	NARX
3	0.968	1.069	0.832	0.966	1.107	0.830	NARX
4	0.990	0.667	0.496	0.982	0.884	0.704	NARX
5	0.974	0.975	0.746	0.982	0.817	0.637	NARX
6	0.955	1.055	0.822	0.955	0.980	0.726	NARX
7	0.937	1.391	1.008	0.928	1.626	1.223	NARX
8	0.966	1.371	1.032	0.973	1.230	0.965	NARX
9	0.877	1.879	1.358	0.870	1.892	1.371	A2S
10	0.960	1.376	1.020	0.971	1.137	0.849	NARX
11	0.963	1.049	0.773	0.964	1.079	0.806	NARX
12	0.987	0.783	0.591	0.985	0.865	0.663	NARX
13	0.970	1.263	0.952	0.963	1.369	1.034	A2S
14	0.939	1.655	1.303	0.937	1.721	1.354	A2S
15	0.928	1.714	1.286	0.971	1.154	0.873	NARX
16	0.955	1.055	0.822	0.955	0.980	0.726	NARX
17	0.970	1.224	0.889	0.980	1.063	0.834	A2S
18	0.972	1.181	0.873	0.968	1.289	1.027	A2S
19	0.983	0.956	0.723	0.982	1.052	0.823	A2S
20	0.985	0.899	0.686	0.988	0.848	0.664	NARX
21	0.987	0.832	0.638	0.969	1.294	0.907	A2S
22	0.987	0.829	0.637	0.960	1.467	1.048	A2S
23	0.965	1.383	1.038	0.985	0.928	0.725	NARX
24	0.991	0.698	0.517	0.993	0.663	0.516	NARX
25	0.986	0.786	0.591	0.986	0.817	0.631	NARX
26	0.951	1.407	1.057	0.968	1.180	0.913	A2S
27	0.991	0.615	0.463	0.995	0.492	0.385	NARX

0.315 °C/decade). Moreover, for each hydrological station, river water temperature warms slower than air temperature with the ratio varying between 0.11 and 0.93 (average: 0.58), which is clearly shown in Fig. 5 as well.

For seasonal trends, as shown in Table 4, spring RWT in 16 out of 27 hydrological stations showed a warming trend ($p < 0.05$) following the warming of air temperature, with the warming rate ranging from 0.267 °C/decade to 0.538 °C/decade (average: 0.379 °C/decade). For summer, RWT in 21 out of 27 hydrological stations showed a warming trend ($p < 0.05$), with the warming rate varying between 0.144 °C/decade and 0.712 °C/decade (average: 0.480 °C/decade). As for autumn, RWT in 22 out of 27 hydrological stations showed a warming trend ($p < 0.05$), with the warming rate varying between 0.229 °C/decade and 0.720 °C/decade (average:

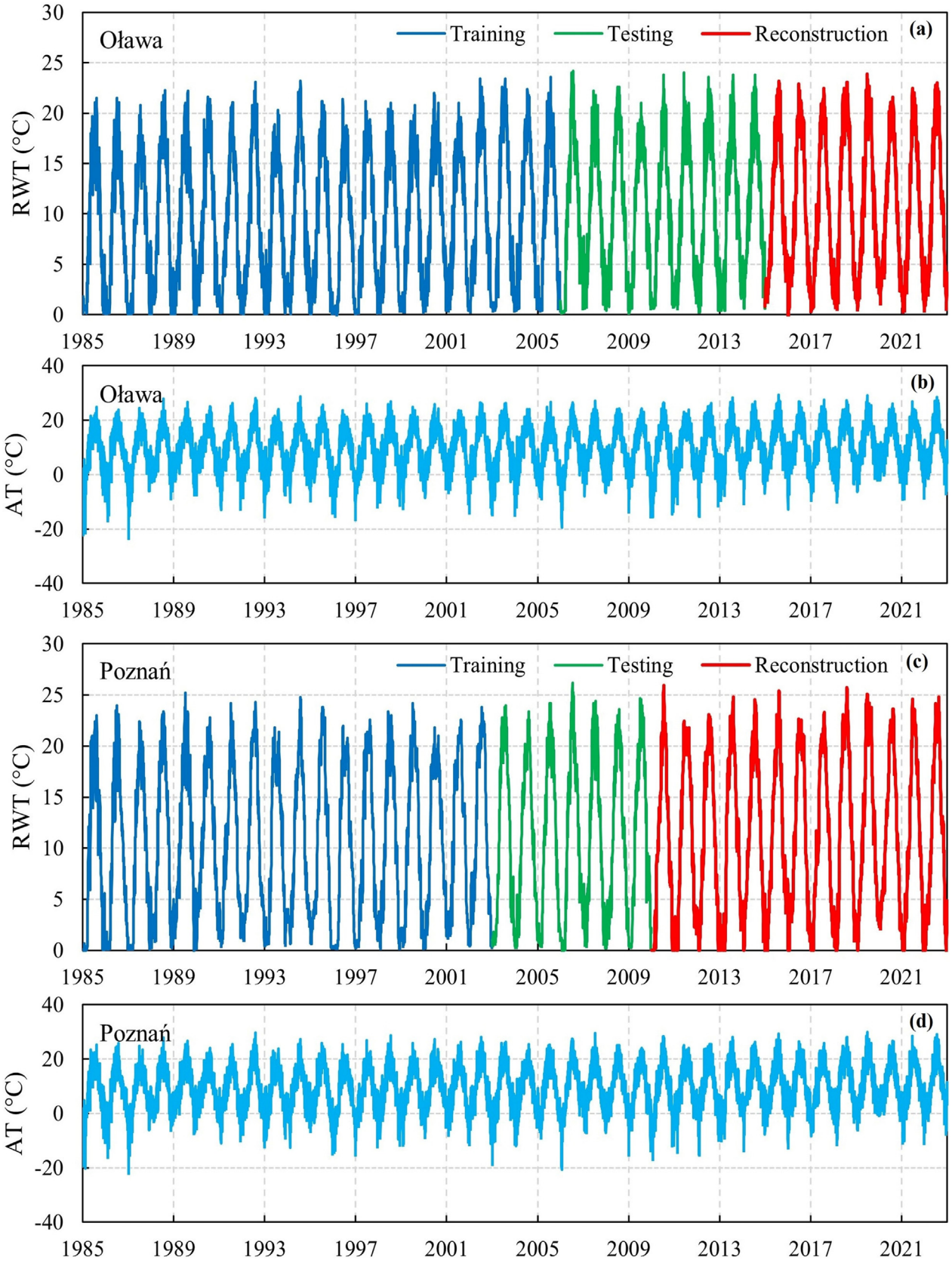

Fig. 3. RWT and AT time series for: Oława (No. 4): (a) RWT and (b) AT; Poznań (No. 19): (c) RWT and (d) AT. The station No. corresponds with that list in Table 1.

0.393 °C/decade). Overall, summer RWT warms faster, followed by autumn and spring. For most of the hydrological stations, seasonal RWT warms slower than air temperature, however, there are still some exceptions, especially for summer. For example, for three sta-

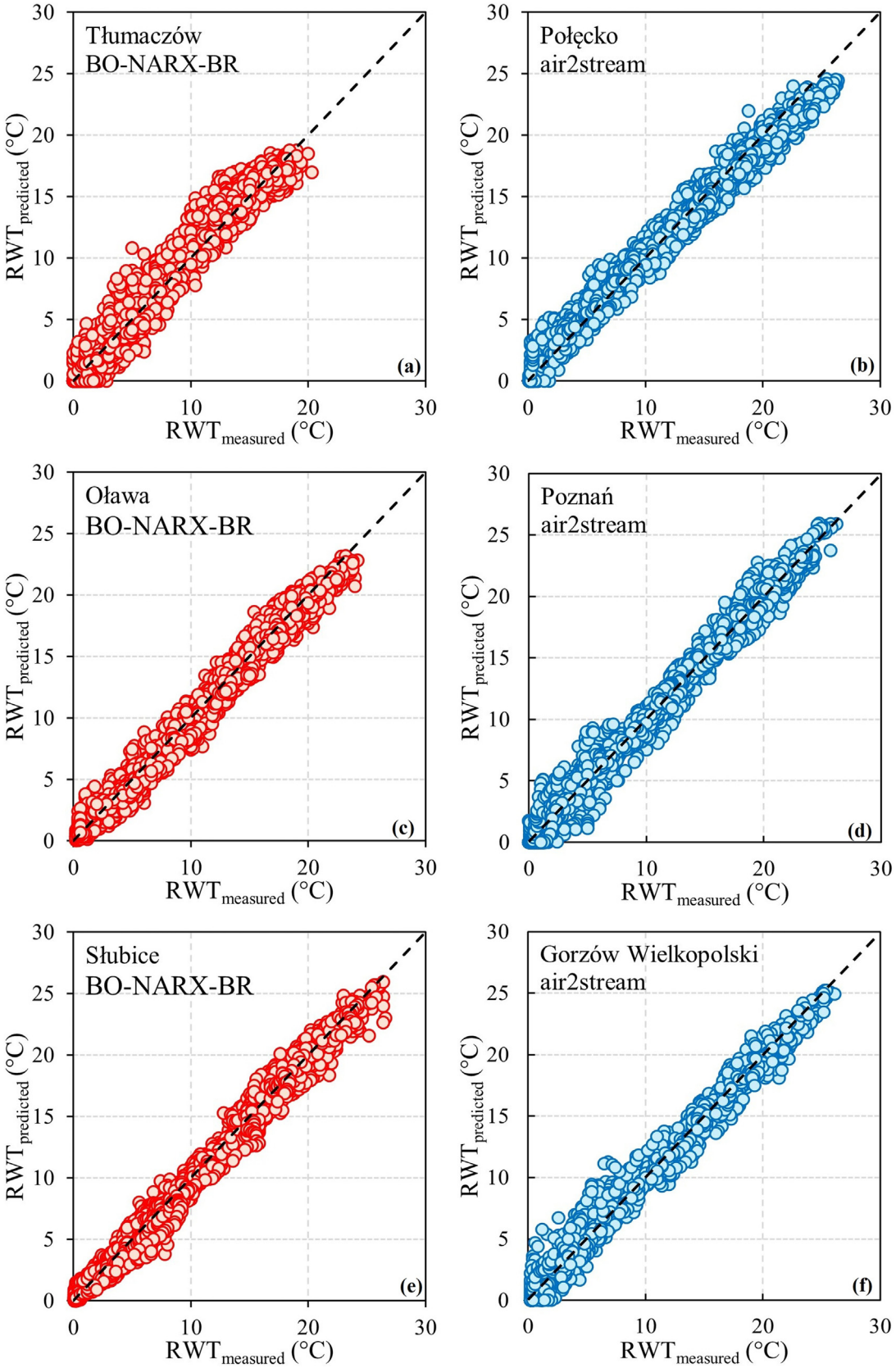

Fig. 4. Measured vs predicted RWT – Testing stage: (a) Tłumaczów (No. 2); (b) Połęcko (No. 17). (c) Oława (No. 4); (d) Poznań (No. 19); (e) Słubice (No. 20); (f) Gorzów Wielkopolski (No. 22).

Table 4
Annual and seasonal warming rates (°C/decade) of river water temperatures and air temperatures. The station No. corresponds with that list in Table 1. RWT is river water temperature, AT is air temperature, and '/' means the varying trend is insignificant ($p > 0.05$).

Station No.	Annual		Spring		Summer		Autunm	
	RWT	AT	RWT	AT	RWT	AT	RWT	AT
1	0.319	0.498	/	0.371	0.391	0.467	0.396	0.623
2	0.054	0.498	/	0.371	/	0.467	0.345	0.623
3	0.363	0.675	0.445	0.600	0.476	0.694	0.366	0.715
4	0.544	0.675	0.538	0.600	0.679	0.694	0.579	0.715
5	0.232	0.544	0.267	0.427	/	0.598	0.298	0.617
6	0.182	0.416	/	0.367	0.144	0.400	0.229	0.476
7	/	0.531	/	0.430	0.571	0.564	0.427	0.591
8	0.363	0.531	/	0.430	0.584	0.564	0.367	0.591
9	0.093	0.549	/	0.529	/	0.577	0.386	0.562
10	0.462	0.538	/	0.459	0.499	0.587	0.720	0.601
11	0.233	0.549	0.406	0.529	/	0.577	/	0.562
12	0.353	0.538	0.327	0.459	0.501	0.587	0.341	0.601
13	0.262	0.518	0.295	0.408	0.375	0.573	0.273	0.580
14	0.191	0.530	0.275	0.495	/	0.585	/	0.545
15	/	0.479	/	0.342	/	0.484	/	0.600
16	0.481	0.518	0.395	0.408	0.637	0.573	0.468	0.580
17	0.290	0.549	0.347	0.529	0.383	0.577	/	0.562
18	0.420	0.549	0.339	0.529	0.538	0.577	0.533	0.562
19	0.439	0.616	0.383	0.555	0.712	0.757	0.417	0.614
20	0.370	0.530	0.450	0.495	0.487	0.585	0.358	0.545
21	0.338	0.530	/	0.503	0.498	0.557	0.356	0.540
22	0.359	0.530	0.308	0.557	0.485	0.503	0.329	0.540
23	0.136	0.505	/	0.418	0.270	0.535	/	0.556
24	0.445	0.530	0.527	0.503	0.529	0.557	0.441	0.540
25	0.355	0.530	0.379	0.503	0.475	0.557	0.378	0.540
26	0.286	0.530	/	0.503	0.353	0.557	0.358	0.540
27	0.311	0.520	0.376	0.446	0.492	0.583	0.285	0.527

tions (Nos. 7, 8, and 16), summer RWT warms faster than air temperature.

Correlation coefficient (r) between seasonal air temperatures and river water temperatures across all hydrological stations is summarized in Supplementary Data Table S3. Specifically, r varies from 0.42 to 0.96 (average: 0.78, Standard Deviation (SD): 0.17) for spring; for summer, r ranges from 0.28 to 0.96 (average: 0.78, SD: 0.18); r has an average value of 0.80 (0.58–0.93, SD: 0.10) for autumn; and for winter, r varies from 0.78 to 0.97 (average: 0.88, SD: 0.06). As shown, air temperature is the main impact factor controlling seasonal RWT for majority of hydrological stations. With the warming of seasonal air temperatures in spring, summer, and autumn, RWT generally tends to increase, as shown above. For winter, as air temperatures showed insignificant warming trends, winter RWT showed an insignificant trend for all hydrological stations. Moreover, as shown from the SD values, spring and summer have relatively larger SD values, as in some hydrological stations (e.g., Tłumaczów), r values are small in these two seasons (Supplementary Data Table S3), indicating that other local conditions (e.g., basin properties) may impact the relationship between seasonal RWT and air temperature (e.g., Tokarczyk, 2013; Laizé et al., 2017).

3.3. River heatwaves

In this study, the number, duration, maximum intensity, and cumulative intensity of river heatwaves were computed for each hydrological station. The trends are presented in Table 5. As seen, for the majority of hydrological stations, river heatwaves are increased in number, duration, and intensity: (i) total number increased at an average rate of 0.814 times/decade, with a range of 0.594–1.516 times/decade; (ii) total duration increased at an average rate of 9.258 d/decade, from 5.608 d/decade to 17.555 d/decade; (iii) maximum intensity increased from 0.201 °C/decade to 0.469 °C/decade, with an average rate of 0.330 °C/decade; and (iv) cumulative intensity increased from 14.329 °C/decade to 46.03 °C/decade, with an average rate of 26.504 °C/decade.

Concerning the category of each heatwave event, which is summarized in Table 6, for each hydrological station, the majority of heatwave events belong to the category 'M' (moderate) with a percentage of around 84.4%, followed by 'S' (strong) with a percentage of around 15.4%, and only a few hydrological stations showed categories of 'SE' (severe) and 'E' (extreme). The category shown in Table 6 indicated that river heatwaves are at moderate to strong levels for the Odra River Basin.

For basin average condition (averaged values of the 27 hydrological stations), the four variables all show clear increasing rate ($p < 0.05$), which is shown in Fig. 6. As seen, total number increased at a rate of 0.706 times/decade, total duration increased at a rate of 7.710 d/decade, maximum intensity increased with a rate of 0.227 °C/decade, and cumulative intensity increased with a rate of 21.190 °C/decade. The results indicated that the overall river heatwaves in the Odra River Basin tend to increase in frequency and intensity.

4. Discussion

4.1. Ensemble modeling

Many studies used a single model for the reconstruction of daily RWT, and the majority of them used the air2stream model due to its simplicity and accuracy (e.g., Zhu et al., 2022; Shrestha and Pesklevits, 2023; Shrestha et al., 2024). However, recent studies showed that the performance of the air2stream model is site-dependent, and the NARX-based model can produce better results in the Vistula River Basin, Europe (Sun et al., 2024; Zhu et al., 2024). For the Odra River Basin investigated in this study (located in the same region as the Vistula River Basin), the modeling results showed that the NARX-based model outperformed the air2stream model in 18 out of the 27 hydrological stations, indicating the overall better performance of the NARX-based model. As shown by Zhu et al. (2024), NARX-based models can accelerate convergence towards optimal weights for connections between neurons

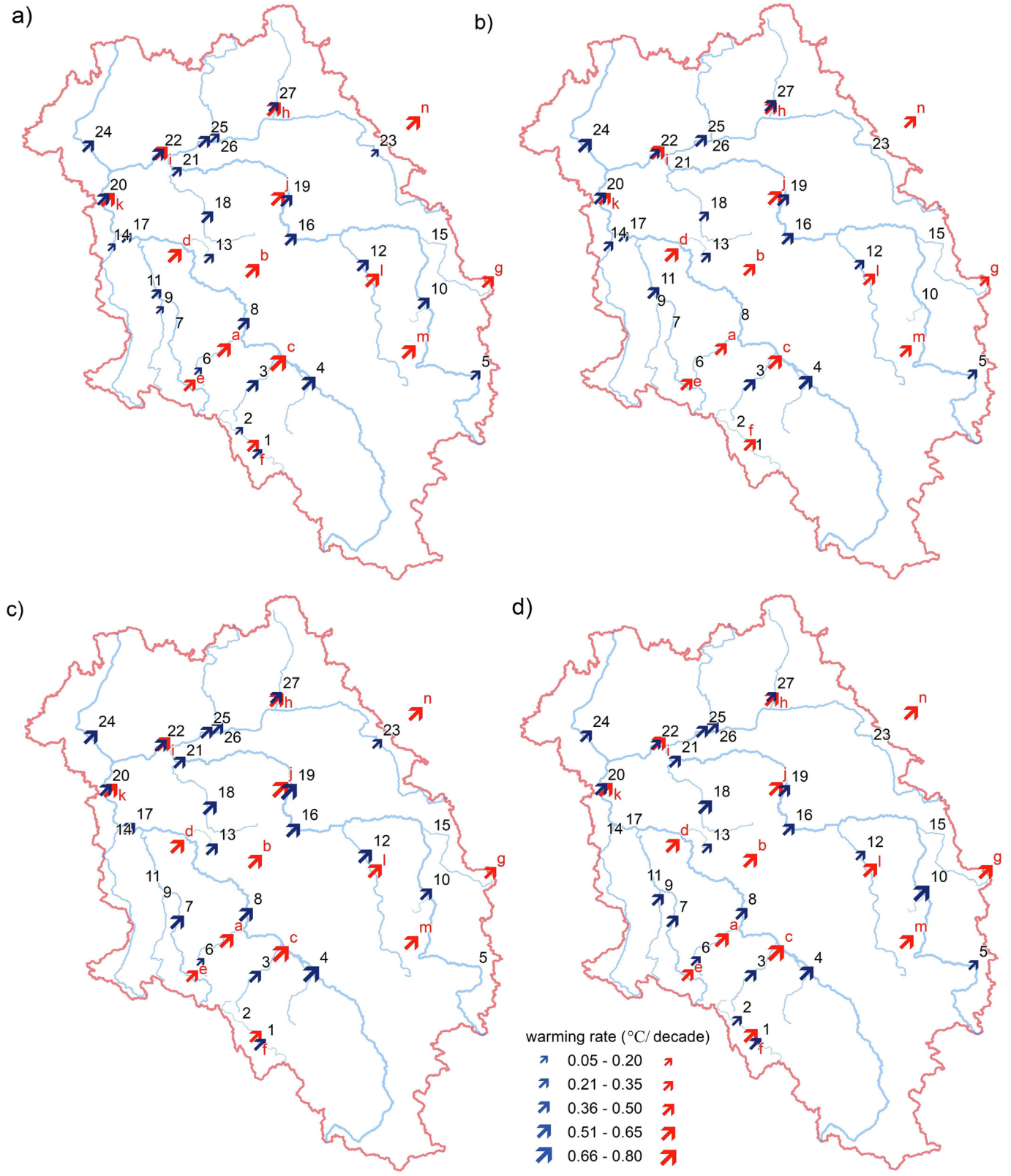

Fig. 5. Warming rates of river water temperatures (blue arrows) and air temperatures (red arrows): (a) annual, (b) spring, (c) summer, and (d) autumn. The station No. corresponds with that list in Table 1. (For interpretation of the references to colour in this figure legend, the reader is referred to the web version of this article.)

and input parameters, and there is a notable reduction in the number of parameters requiring calibration to enhance the model's effectiveness, making them prominent for RWT modeling. For the 9 hydrological stations where the air2stream model performed relatively better, observed RWT data are not complete, which might impact the determination of the delays of the NARX-based model (Table 2), thus affecting the performance of the NARX-based model.

Table 5
Trends of river heatwaves. The station No. corresponds with that list in Table 1. '/' means the varying trend is insignificant ($p > 0.05$).

Station No.	Number (times/decade)	Duration (days/decade)	Maximum intensity (°C/decade)	Cumulative intensity (°C/decade)
1	/	/	/	/
2	/	/	/	/
3	1.088	9.164	0.469	32.830
4	1.516	13.782	0.377	46.030
5	/	/	/	/
6	/	/	/	/
7	/	/	/	/
8	0.710	17.555	/	32.681
9	/	/	/	/
10	/	/	/	/
11	0.867	7.460	0.263	17.602
12	0.727	5.608	/	18.877
13	/	/	/	/
14	0.710	9.282	/	15.508
15	/	/	/	/
16	0.594	8.765	/	30.036
17	0.725	7.295	/	20.716
18	0.687	7.317	/	23.135
19	/	9.134	/	32.475
20	0.854	11.605	0.411	35.139
21	0.631	8.283	/	27.656
22	0.762	7.988	/	27.155
23	0.661	7.800	/	22.319
24	0.701	7.353	0.275	23.584
25	1.017	12.776	0.201	32.849
26	0.688	7.344	/	14.329
27	0.892	8.125	0.311	24.152

Table 6
Summary of the number of each category for each hydrological station. The station No. corresponds with that list in Table 1. 'M' (moderate), 'S' (strong), 'SE' (severe), and 'E' (extreme).

Station No.	Total number	M	S	SE	E
1	93	65	27	1	0
2	118	102	16	0	0
3	104	77	27	0	0
4	115	86	28	1	0
5	98	78	20	0	0
6	97	79	18	0	0
7	96	82	12	1	1
8	94	84	10	0	0
9	104	89	15	0	0
10	106	87	19	0	0
11	100	84	16	0	0
12	116	100	16	0	0
13	94	77	17	0	0
14	119	103	15	1	0
15	79	65	14	0	0
16	132	110	22	0	0
17	128	111	16	1	0
18	129	111	17	1	0
19	120	106	14	0	0
20	119	102	17	0	0
21	127	112	15	0	0
22	113	101	12	0	0
23	118	95	23	0	0
24	119	109	10	0	0
25	123	115	8	0	0
26	121	108	13	0	0
27	127	110	17	0	0

Ensemble modeling by combining the two models can improve the reliability of the results. For example, compared with Zhu et al. (2022), which employed only the air2stream model to reconstruct daily RWT in Polish rivers, the results in this study are better, e.g., average RMSE values for the training and testing periods are 1.165 °C and 1.129 °C respectively in this study, and are 1.21 °C and 1.32 °C in Zhu et al. (2022). The results suggest that ensemble modeling by combining multiple models is a better choice for the reconstruction of daily RWT. Previously, Sojka and Ptak (2022) attempted to reconstruct monthly mean river water temperatures using multiple linear regression, multilayer perceptron network and random forest regression, and the results showed that the multilayer perceptron network was best suited for this purpose, obtaining an average RMSE of 0.5 °C. However, it is not possible to analyze river heatwaves as with the reconstruction of daily RWT like in this study.

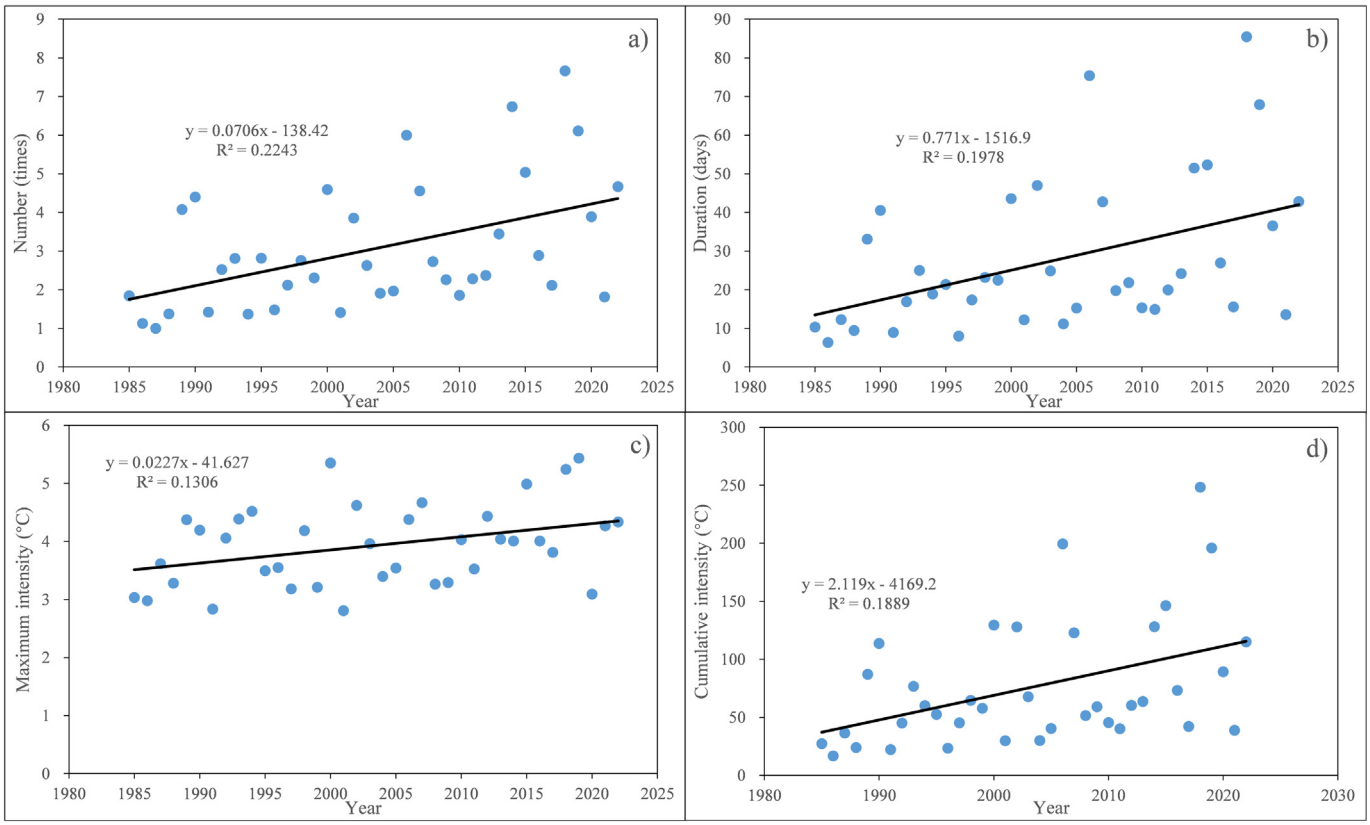

Fig. 6. Trends of river heatwaves for basin averaged values: (a) number, (b) duration, (c) maximum intensity, and (d) cumulative intensity.

4.2. Warming trends of river water temperatures

Rivers are extremely susceptible to any changes that take place in the environment which is reflected both in the amount of water but also in the course of physical and chemical parameters. In an era of global warming, increasing attention is being focused on the scale and rate of change in water temperature, which is crucial to these ecosystems. Numerous studies conducted in different regions of the world prove that there is a change in the thermal regime of rivers (Kaushal et al., 2010; Chen et al., 2016; Zabolotnia, 2018; Itsukushima et al., 2024). Webb (1996) indicated that there was a warming of the average temperature of rivers in Europe during the 20th Century of about 1 °C. This trend was not continuous which is due to extreme hydrological events. On the other hand, analyzing previous studies in the area of the present research, thus relating to Central Europe, it can be said that the results obtained are in line with them.

For example, Ptak et al. (2022) showed that the Vistula River is warming at an average rate of 0.31 °C/decade; Niedrist (2023) showed that Central European mountain rivers are warming at a rate between 0.24 °C/decade and 0.44 °C/decade. Upward trends in water temperatures ranging from 0.10 °C/decade to 0.54 °C/decade have been shown in rivers located in the catchment area of the Warta River (Gizińska and Sojka, 2023). For the five coastal rivers in the southern Baltic Sea zone, water temperature increased in the range of 0.26 °C/decade to 0.31 °C/decade (Ptak et al., 2016). The warming rate computed from the reconstructed data showed that the Odra River is warming at an average rate of 0.315 °C/decade, comparable with previous studies. The increase in water temperature is important for hydrobiological conditions and also affects issues relating to pollution or eutrophication (Johnson et al., 2024). The Odra River and the Vistula River, are the main suppliers of pollution to the Baltic Sea (Schernewski and Neumann, 2002). Against this background, knowing the scale of changes in water temperature is key information for undertaking remedial work relevant not only to the river network located in this basin but of international importance.

4.3. Characteristics of river heatwaves

Analyzing the possible drivers behind the increasing frequency, duration, and intensity of river heatwaves in the Odra River Basin, it was found that air temperature is the major controller. Table 7 summarizes the correlation coefficient (r) between annual air temperatures and the number, duration, and total cumulative intensity of river heatwaves. As seen, for all hydrological stations, the number, duration, and total cumulative intensity of river heatwaves correlated with air temperatures ($p < 0.05$). Specifically, r varied from 0.31 to 0.74 with an average value of 0.61 for the number, r ranged from 0.34 to 0.76 with an average value of 0.62 for the duration, and r varied from 0.26 to 0.76 with an average value of 0.60 for the total cumulative intensity. The results suggest that with the warming of air temperatures, there will be more intensified river heatwaves. Other factors, e.g., land use and land cover, and hydrological regime may impact river heatwaves, however, due to the limitation of these data, their impacts are not analyzed in this study. This issue can be solved once the data about land use and land cover are collected.

4.4. Potential ecological impacts of water temperature changes and heatwave intensification

With global climate change and the increase of extreme climatic events, inland waters are warming, and heatwaves are increasing in frequency and intensity for many water bodies worldwide. For example, Woolway et al. (2021) showed that lake

Table 7
Correlation coefficient (r) between annual air temperatures and number, duration, and total cumulative intensity of river heatwaves.

Station No.	Total cumulative intensity	Duration	Number
1	0.63	0.66	0.67
2	0.55	0.56	0.57
3	0.71	0.73	0.73
4	0.66	0.68	0.74
5	0.60	0.61	0.57
6	0.52	0.54	0.53
7	0.51	0.56	0.60
8	0.67	0.69	0.66
9	0.52	0.53	0.49
10	0.60	0.61	0.65
11	0.60	0.61	0.64
12	0.67	0.67	0.66
13	0.26	0.34	0.40
14	0.64	0.66	0.61
15	0.31	0.34	0.31
16	0.62	0.62	0.50
17	0.63	0.64	0.62
18	0.64	0.65	0.62
19	0.67	0.69	0.62
20	0.76	0.76	0.73
21	0.62	0.63	0.54
22	0.60	0.61	0.65
23	0.57	0.59	0.61
24	0.67	0.67	0.66
25	0.68	0.69	0.69
26	0.67	0.69	0.65
27	0.69	0.68	0.68

heatwaves will become hotter and longer due to the impact of climate change on global lakes. Wang et al. (2023) demonstrated that climate change drives rapid warming and increasing heatwaves of lakes in China. For rivers, Tassone et al. (2023) found increasing heatwave frequency in streams and rivers in the United States. Zhu et al. (2024) found that river heatwaves have increased in frequency and intensity for the Vistula River Basin, Europe. Using the reconstructed RWT dataset for the computation of river heatwaves, the results in this study showed that river heatwaves increased in number, duration, and intensity for the Odra River Basin with the increase in air temperatures. Notably, most of the heatwave events are moderate to strong, with only a few exceptions (severe and extreme). In the case of rivers, commonly considered extreme situations refer to floods and droughts (Vicente-Serrano et al., 2017; Sánchez-García and Francos, 2022; Gao et al., 2024). However, given the elemental importance of water temperature, it can be concluded that heatwaves will be crucial to the properties of river ecosystems. Adapting to extreme hydrological events and subsequently responding appropriately to mitigate their effects requires accurate and reliable risk assessment and understanding (Nguma and Kiluva, 2022). The results obtained in this study enrich the knowledge in this area while indicating the need for similar analyses for other catchments.

Studies have shown that warming of RWT can cause deoxygenation in rivers (e.g., Zhi et al., 2023b), pose adverse impacts on aquatic life, and aggravate pervasive issues such as eutrophication, pollution, and the spread of disease, as summarized in Thompson et al. (2021) and Johnson et al. (2024). In this regard, the observed water temperature changes and heatwave intensification might induce potential ecological impacts on the Odra River Basin (e.g., deoxygenation), though there are no specific studies on this topic. This, on the other hand, suggests that more in-depth studies combining field observation and modeling are needed to investigate the impacts of water temperature changes and heatwave intensification on the Odra River Basin, which can be enhanced once more water quality data are available. Detailed knowledge of water temperature as an elemental characteristic of water is important for many reasons, including considering at least the events of 2022. That summer, a mass die-off of organisms occurred on the Oder River, which was attributed to toxins released by Prymnesium parvum (Szlauer-Łukaszewska et al., 2024). According to Sobieraj and Metelski (2023), the disaster occurred as a result of significant changes in water parameters (indicating, among other things, increased water temperature) and a significant degree of hydromorphological changes in the river.

4.5. Mitigation strategies and their documented effectiveness

The results in this study indicated that mitigation measures are needed to reduce the impact of climate change on the studied basin. Previous studies showed that the presence of trees near the river (riparian shading) is important for reducing water temperature (Pedreros et al., 2016; Trimmel et al., 2018; Cunningham et al., 2023), and flow management by optimal dam operations can act as thermal protection to warming and heatwave effects (e.g., Renöfält et al., 2010; Feng et al., 2018; Tassone et al., 2023). In the case of the Odra River Basin, there was a positive effect of forested areas. Analysis of the thermal conditions in two smaller catchments (Czerna Wielka and Szprotawa) revealed differences of 1.2 °C in average annual temperatures. During the growing season, this difference increased to 2.6 °C (Ptak, 2017). Therefore, it is worth considering future appropriate management of riparian zones, especially for small rivers, where shaded areas can significantly impact river temperatures.

4.6. Potential applications of the models in quantifying trends in river water temperatures and heatwaves under different climate change scenarios

The impact of future climate on river thermal dynamics and heatwaves can be investigated by combining the models used in this study and scenarios of climate models. Models like NARX and air2stream can be effectively used by leveraging their ability to incorporate complex, nonlinear relationships and external climate variables. NARX models are particularly suited for this task due to their structure, which integrates past values of the time series (e.g., historical river temperatures) along with exogenous inputs (e.g., air temperatures) to predict future values. This allows them to capture the intricate dynamics between river water temperatures and climate variables. The air2stream model, which is specifically designed to relate air temperatures to water temperatures, can complement this by providing a focused mechanism to project how changes in air temperature, a key aspect of climate change, directly influence river water temperatures. Firstly, daily air temperature data under different climate change scenarios can be obtained from climate models. For Poland, the EURO-CORDEX project is a good choice. These data need to be calibrated to historical periods, to make sure that they have enough accuracy for the study region. Then, the calibrated models can be used to project future river water temperatures for each hydrological station by using these air temperature data as model input. Finally, trends in river water temperatures and the frequency and intensity of heatwaves under various climate change scenarios can be deduced by analyzing the projected time series data generated by these models.

5. Conclusions

In this study, ensemble models by combining NARX and air2stream, were used to reconstruct daily river water temperatures in the Odra River Basin, one of the largest river systems in Europe. The results lead to the following conclusions:

(i) Ensemble modeling by combining NARX and air2stream is a valuable tool for reconstructing daily river water temperatures.

(ii) Annual RWT showed a significant warming trend over the past 40 years with an average warming rate of 0.315 °C/decade. Seasonal RWT indicated that summer warms faster, followed by autumn and spring, and winter RWT showed an insignificant warming trend.

(iii) River heatwaves are increased in frequency, duration, and intensity in the Odra River Basin. The majority of river heatwave events are categorized as 'moderate' and 'strong', suggesting that mitigation measures are needed to reduce the impact of climate warming on aquatic systems. With the warming of air temperatures, river heatwaves tend to intensify.

CRediT authorship contribution statement

Jiang Sun: Writing – review & editing, Writing – original draft, Methodology, Investigation. **Fabio Di Nunno:** Writing – review & editing, Writing – original draft, Visualization, Validation, Methodology, Investigation. **Mariusz Sojka:** Writing – review & editing, Writing – original draft, Data curation. **Mariusz Ptak:** Writing – review & editing, Writing – original draft, Data curation. **Quan Zhou:** Writing – review & editing, Writing – original draft. **Yi Luo:** Writing – review & editing, Writing – original draft, Funding acquisition. **Senlin Zhu:** Writing – review & editing, Writing – original draft, Supervision, Methodology, Investigation, Conceptualization. **Francesco Granata:** Writing – review & editing, Writing – original draft, Validation, Supervision, Methodology, Investigation.

Data availability

The codes of the BO-NARX-BR model are available at: https://github.com/Fabiodinunno1989/LSWT-prediction/tree/main. The observed data are available upon reasonable request from the corresponding author.

Declaration of competing interest

The authors declare that they have no known competing financial interests or personal relationships that could have appeared to influence the work reported in this paper.

Acknowledgements

The authors acknowledge the Institute of Meteorology and Water Management–National Research Institute in Poland for providing the data used in this study. This study is funded by the National Science Foundation of China (Grant No. 42401572), Natural Science Foundation of the Jiangsu Higher Education Institutions of China (Grant No. 22KJB170023) and Postgraduate Research & Practice Innovation Program of Jiangsu Province (No. KYCX24_3758).

Appendix A. Supplementary data

Supplementary data to this article can be found online at https://doi.org/10.1016/j.gsf.2024.101916.

References

Almeida, M.C., Coelho, P.S., 2023. Modeling river water temperature with limiting forcing data: air2stream v1. 0.0, machine learning and multiple regression. Geosci. Model Dev. 16 (14), 4083–4112.

Bal, G., de Eyto, E., 2023. Simple Bayesian reconstruction and forecasting of stream water temperature for ecologists—a tool using air temperature, optionally flow, in a time series decomposition approach. PLoS One 18 (9), e0291239.

Benyahya, L., Caissie, D., St-Hilaire, A., Ouarda, T.B., Bobée, B., 2007. A review of statistical water temperature models. Can. Water Resour. J. 32 (3), 179–192.

Caissie, D., 2006. The thermal regime of rivers: a review. Freshw. Biol. 51 (8), 1389–1406.

Chen, D., Hu, M., Guo, Y., Dahlgren, R.A., 2016. Changes in river water temperature between 1980 and 2012 in Yongan watershed, eastern China: magnitude, drivers and models. J. Hydrol. 533, 191–199.

Cunningham, D.S., Braun, D.C., Moore, J.W., Martens, A.M., 2023. Forestry influences on salmonid habitat in the North Thompson River watershed, British Columbia. Can. J. Fish. Aquat. Sci. 80 (7), 1053–1070.

Di Nunno, F., Race, M., Granata, F., 2022. A nonlinear autoregressive exogenous (NARX) model to predict nitrate concentration in rivers. Environ. Sci. Pollut. Res. 29, 40623–40642.

Di Nunno, F., Zhu, S., Ptak, M., Sojka, M., Granata, F., 2023. A stacked machine learning model for multi-step ahead prediction of lake surface water temperature. Sci. Total Environ. 890, 164323.

Dion, P., Martel, J.L., Arsenault, R., 2021. Hydrological ensemble forecasting using a multi-model framework. J. Hydrol. 600, 126537.

Duan, Q., Ajami, N.K., Gao, X., Sorooshian, S., 2007. Multi-model ensemble hydrologic prediction using Bayesian model averaging. Adv. Water Resour. 30 (5), 1371–1386.

Dugdale, S.J., Hannah, D.M., Malcolm, I.A., 2017. River temperature modelling: a review of process-based approaches and future directions. Earth Sci. Rev. 175, 97–113.

Feigl, M., Lebiedzinski, K., Herrnegger, M., Schulz, K., 2021. Machine learning methods for stream water temperature prediction. Hydrol. Earth Syst. Sci. 25, 2951–2977.

Feng, M., Zolezzi, G., Pusch, M., 2018. Effects of thermopeaking on the thermal response of alpine river systems to heatwaves. Sci. Total Environ. 612, 1266–1275.

Foresee, F.D, Hagan, M.T. 1997. Gauss-Newton approximation to Bayesian learning. In: Proceedings of the International Joint Conference on Neural Networks.

Gao, G., Li, J., Feng, P., Liu, J., Wang, Y., 2024. How extreme hydrological events correspond to climate extremes in the context of global warming: a case study in the Luanhe River Basin of North China. Int. J. Climatol. 44 (7), 2391–2405. https://doi.org/10.1002/joc.8459.

Gizińska, J., Sojka, M., 2023. How climate change affects river and lake water temperature in Central-West Poland—A case study of the Warta River Catchment. Atmosphere 14, 330.

Hobday, A.J., Alexander, L.V., Perkins, S.E., Smale, D.A., Straub, S.C., Oliver, E.C., Benthuysen, J.A., Burrows, M.T., Donat, M.G., Feng, M., Holbrook, N.J., 2016. A hierarchical approach to defining marine heatwaves. Prog. Oceanogr. 141, 227–238.

Huang, F., Qian, B., Ochoa, C.G., 2023. Long-term river water temperature reconstruction and investigation: a case study of the Dongting Lake Basin, China. J. Hydrol. 616, 128857.

Itsukushima, R., Ohtsuki, K., Sato, T., 2024. Drivers of rising monthly water temperature in river estuaries. Limnol. Oceanogr. 69 (3), 589–603.

Johnson, M.F., Albertson, L.K., Algar, A.C., Dugdale, S.J., Edwards, P., England, J., Gibbins, C., Kazama, S., Komori, D., MacColl, A.D., Scholl, E.A., 2024. Rising water temperature in rivers: ecological impacts and future resilience. Wiley Interdiscip. Rev.: Water, e1724.

Kaushal, S.S., Likens, G.E., Jaworski, N.A., Pace, M., Sides, A.M., Seekell, D., Belt, K.T., Secor, D.H., Wingate, R.L., 2010. Rising stream and river temperatures in the United States. Front. Ecol. Environ. 8 (9), 461–466.

Laizé, C.L., Bruna Meredith, C., Dunbar, M.J., Hannah, D.M., 2017. Climate and basin drivers of seasonal river water temperature dynamics. Hydrol. Earth Syst. Sci. 21 (6), 3231–3247.

MacKay, D.J.C., 1992. Bayesian Interpolation. Neural Comput. 4, 415–447.

Mohseni, O., Stefan, H.G., 1999. Stream temperature/air temperature relationship: a physical interpretation. J. Hydrol. 218, 128–141.

Nguma, R.K., Kiluva, V.M. 2022. Management of extreme hydrological events. Climate Impacts on Extreme Weather: Current to Future Changes on a Local to Global Scale, 271-2861.

Niedrist, G.H., 2023. Substantial warming of Central European mountain rivers under climate change. Reg. Environ. Chang. 23 (1), 43.

Olsson, F., Moore, T.N., Carey, C.C., Breef-Pilz, A., Thomas, R.Q., 2024. A multi-model ensemble of baseline and process-based models improves the predictive skill of near-term lake forecasts. Water Resour. Res. 60 (3). e2023WR035901.

Pedreros, P., Guevara-Mora, M., Urrutia, R., Stehr, A., 2016. The importance of Nothofagus dombeyi (Mirb.) Oerst. riparian vegetation in the thermal regime of Andean streams of Southern Chile. Gayana - Botanica 73 (1), 32–41.

Ptak, M., 2017. Wpływ zalesienia na temperaturę wody w rzece. Leśne Prace Badawcze 78 (3), 251–256.

Ptak, M., Choiński, A., Kirviel, J., 2016. Long-term water temperature fluctuations in coastal rivers (Southern Baltic) in Poland. Bull. Geogr. Phys. Geogr. Ser. 11, 35–42.

Ptak, M., Sojka, M., Graf, R., Choiński, A., Zhu, S., Nowak, B., 2022. Warming Vistula River–the effects of climate and local conditions on water temperature in one of the largest rivers in Europe. J. Hydrol. Hydromech. 70 (1), 1–11.

Qiu, R., Wang, Y., Rhoads, B., Wang, D., Qiu, W., Tao, Y., Wu, J., 2021. River water temperature forecasting using a deep learning method. J. Hydrol. 595, 126016.

Renöfält, B.M., Jansson, R., Nilsson, C., 2010. Effects of hydropower generation and opportunities for environmental flow management in Swedish riverine ecosystems. Freshw. Biol. 55 (1), 49–67.
Sánchez-García, C., Francos, M., 2022. Human-environmental interaction with extreme hydrological events and climate change scenarios as background. Geogr. Sustain. 3 (3), 232–236.
Schernewski, G., Neumann, T. 2002. Perspectives on eutrophication abatement in the Baltic Sea, in Littoral 2002: The Changing Coast, Vol. 2, ed. EUROCOAST/EUCC (Portugal: EUROCAST), 503-511.
Shrestha, R.R., Pesklevits, J.C., 2023. Reconstructed river water temperature dataset for Western Canada 1980–2018. Data 8 (3), 48.
Shrestha, R.R., Pesklevits, J.C., Bonsal, B.R., Brannen, R., Guo, T., Hoffman, S., 2024. Rising summer river water temperature across Canada: spatial patterns and hydroclimatic controls. Environ. Res. Lett. 19, 044058.
Sobieraj, J., Metelski, D., 2023. Insights into toxic Prymnesium parvum blooms as a cause of the ecological disaster on the Odra river. Toxins 15, 403.
Sojka, M., Ptak, M., 2022. Possibilities of river water temperature reconstruction using statistical models in the context of long-term thermal regime changes assessment. Appl. Sci. 12 (15), 7503.
Stefan, H.G., Preud'homme, E.B., 1993. Stream temperature estimation from air temperature. J. Am. Water Resour. Assoc. 29 (1), 27–45.
Sun, J., Di Nunno, F., Sojka, M., Ptak, M., Luo, Y., Xu, R., Xu, J., Luo, Y., Zhu, S., Granata, F., 2024. Prediction of daily river water temperatures using an optimized model based on NARX networks. Ecol. Ind. 161, 111978.
Szlauer-Łukaszewska, A., Ławicki, Engel, J., Drewniak, E., Ciężak, K., Marchowski, D., 2024. Quantifying a mass mortality event in freshwater wildlife within the Lower Odra River: Insights from a large European river. Sci. Total Environ. 907, 167898.
Tao, Y., Wang, Y., Wang, D., Ni, L., Wu, J., 2021. A C-vine copula framework to predict daily water temperature in the Yangtze River. J. Hydrol. 598, 126430.
Tassone, S.J., Besterman, A.F., Buelo, C.D., Ha, D.T., Walter, J.A., Pace, M.L., 2023. Increasing heatwave frequency in streams and rivers of the United States. Limnol. Oceanogr. Lett. 8 (2), 295–304.
Thompson, J.R., Gosling, S.N., Zaherpour, J., Laizé, C.L.R., 2021. Increasing risk of ecological change to major rivers of the world with global warming. Earth's Future 9 (11). e2021EF002048.
Tockner, K., Tonolla, D., Bremerich, V., Jahnig, S.C., Robinson, C.T., Zarfl, C., 2022. Introduction to European Rivers. In: Tockner, K., Zarfl, C., Robsinson, C.T. (Eds.), Rivers of Europe. Elsevier, London, pp. 1–26.
Toffolon, M., Piccolroaz, S., 2015. A hybrid model for river water temperature as a function of air temperature and discharge. Environ. Res. Lett. 10 (11), 114011.
Tokarczyk, T., 2013. Classification of low flow and hydrological drought for a river basin. Acta Geophys. 61 (2), 404–421.
Trimmel, H., Weihs, P., Leidinger, D., Formayer, H., Kalny, G., Melcher, A., 2018. Can riparian vegetation shade mitigate the expected rise in stream temperatures due to climate change during heat waves in a human-impacted pre-alpine river? Hydrol. Earth Syst. Sci. 22 (1), 437–461.
Velázquez, J.A., Anctil, F., Perrin, C., 2010. Performance and reliability of multimodel hydrological ensemble simulations based on seventeen lumped models and a thousand catchments. Hydrol. Earth Syst. Sci. 14 (11), 2303–2317.
Vicente-Serrano, S.M., Zabalza-Martínez, J., Borràs, G., López-Moreno, J.I., Pla, E., Pascual, D., Savé, R., Biel, C., Funes, I., Azorin-Molina, C., Tomas-Burguera, M., El Kenawy, A., 2017. Extreme hydrological events and the influence of reservoirs in a highly regulated river basin of northeastern Spain. J. Hydrol.: Reg. Stud. 12, 13–32.
Wang, X., Shi, K., Zhang, Y., Qin, B., Zhang, Y., Wang, W., Woolway, R.I., Piao, S., Jeppesen, E., 2023. Climate change drives rapid warming and increasing heatwaves of lakes. Sci. Bull. 68 (14), 1574–1584.
Webb, B.W., 1996. Trends in stream and river temperature. Hydrol. Process. 10 (2), 205–226.
Woolway, R.I., Jennings, E., Shatwell, T., Golub, M., Pierson, D.C., Maberly, S.C., 2021. Lake heatwaves under climate change. Nature 589 (7842), 402–407.
Wright, S.A., Anderson, C.R., Voichick, N., 2009. A simplified water temperature model for the Colorado River below Glen Canyon Dam. River Res. Appl. 25 (6), 675–686.
Zabolotnia, T., 2018. Estimation of the long-term tendencies and homogeneity of the average annual water temperature and air temperature in the Siverskyi Donets River Basin (within Ukraine). J. Fund. Appl. Sci. 10, 1–22.
Zhi, W., Klingler, C., Liu, J., Li, L., 2023a. Widespread deoxygenation in warming rivers. Nat. Clim. Chang. 13 (10), 1105–1113.
Zhi, W., Ouyang, W., Shen, C., Li, L., 2023b. Temperature outweighs light and flow as the predominant driver of dissolved oxygen in US rivers. Nat. Water 1 (3), 249–260.
Zhu, S., Luo, Y., Graf, R., Wrzesiński, D., Sojka, M., Sun, B., Kong, L., Ji, Q., Luo, W., 2022. Reconstruction of long-term water temperature indicates significant warming in Polish rivers during 1966–2020. J. Hydrol.: Reg. Stud. 44, 101281.
Zhu, S., Di Nunno, F., Ptak, M., Sojka, M., Granata, F., 2023. A novel optimized model based on NARX networks for predicting thermal anomalies in Polish lakes during heatwaves, with special reference to the 2018 heatwave. Sci. Total Environ. 905, 167121.
Zhu, S., Di Nunno, F., Sun, J., Sojka, M., Ptak, M., Granata, F., 2024. An optimized NARX-based model for predicting thermal dynamics and heatwaves in rivers. Sci. Total Environ. 926, 171954.
Zhu, S., Piotrowski, A.P., 2020. River/stream water temperature forecasting using artificial intelligence models: a systematic review. Acta Geophys. 68, 1433–1442.